JACS
JOURNAL OF THE AMERICAN CHEMICAL SOCIETY

Communication

Superconductivity Induced by Co-Doping in Quaternary Fluoroarsenide CaFeAsF

Satoru Matsuishi, Yasunori Inoue, Takatoshi Nomura, Hiroshi Yanagi, Masahiro Hirano, and Hideo Hosono

J. Am. Chem. Soc., **2008**, 130 (44), 14428-14429 • DOI: 10.1021/ja806357j • Publication Date (Web): 09 October 2008

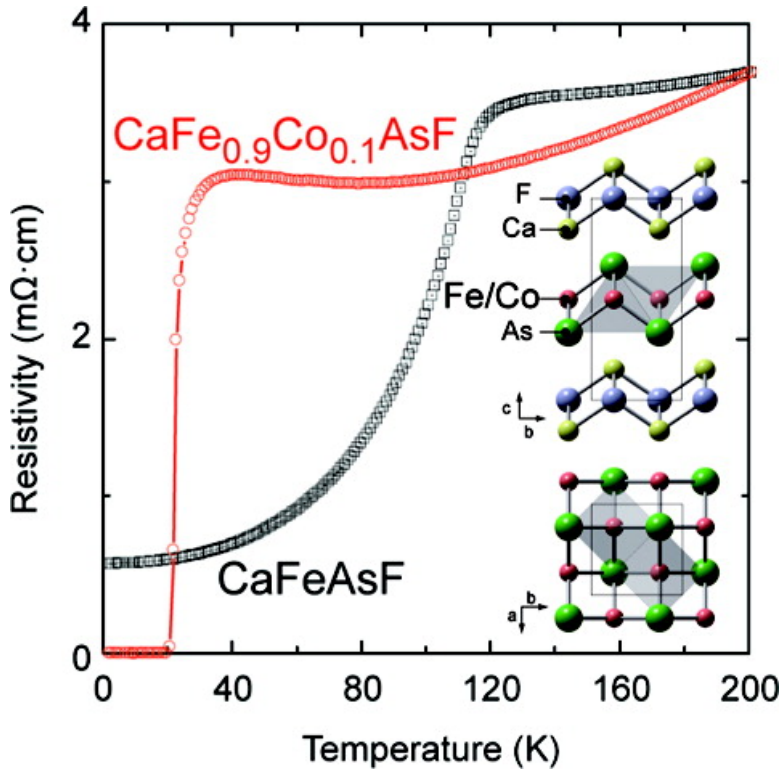

More About This Article

Additional resources and features associated with this article are available within the HTML version:

- Supporting Information
- Access to high resolution figures
- Links to articles and content related to this article

Journal of the American Chemical Society is published by the American Chemical Society. 1155 Sixteenth Street N.W., Washington, DC 20036

J|A|C|S COMMUNICATIONS

Published on Web 10/09/2008

Superconductivity Induced by Co-Doping in Quaternary Fluoroarsenide CaFeAsF

Satoru Matsuishi,*,† Yasunori Inoue,‡ Takatoshi Nomura,‡ Hiroshi Yanagi,‡ Masahiro Hirano,†,§ and Hideo Hosono†,‡,§

Frontier Research Center, Materials and Structures Laboratory, and ERATO-SORST, JST, Tokyo Institute of Technology, 4259 Nagatsuta, Midori-ku, Yokohama 226-8503, Japan

Received August 11, 2008; E-mail: satoru@lucid.msl.titech.ac.jp

Since the discovery of superconductivity in F-doped LaFeAsO with $T_c = 26$ K,[1] FeAs-based layered compounds including *R*FeAsO (*R* = rare-earth)[2−8] and AFe_2As_2 (*A* = alkali-earth)[9−11] have been intensively studied as candidates for high-T_c superconductors. With these efforts, T_c is raised to 56 K in Th-doped GdFeAsO.[8] The parent compounds for these superconductors consist of an $(FeAs)^{\delta-}$ layer forming a square iron lattice sandwiched by $(RO)^{\delta+}$ or $A^{\delta+}$ layers and suffer the crystallographic transition from the tetragonal to orthorhombic, stabilizing the antiferromagnetic spin order at 140−200 K.[1,3,9−13] High concentration doping of the electron or hole to the $(FeAs)^{\delta-}$ layer through the doping of fluorine to $(RO)^{\delta+}$ or alkali-metal to $A^{\delta+}$ layers suppresses the crystallographic and magnetic phase transitions and causes the superconductivity. Therefore, the relation among the structural and magnetic instabilities and superconductivity has been studied, and it was recently found that the superconductivity coexists with the orthorhombic and/or magnetic phases in SmFeAsO for low concentration doping.[14] Further, much effort has been made for the synthesis of related compounds composed of the similar iron lattice with a hope to raise the T_c.[15−18]

Here, we report the synthesis of a new quaternary fluoroarsenide CaFeAsF with the ZrCuSiAs-type structure (space group: *P*4/*nmm*), in which the $(RO)^{\delta+}$ layers in *R*FeAsO are replaced by $(CaF)^{\delta+}$ layers (inset of Figure 1a). This compound exhibits superconductivity by partial replacement of Fe with Co, which is regarded as direct electron doping to the $(FeAs)^{\delta+}$ layer. It is noteworthy that T_c = 22 K is realized for a high Co content of 10% ($CaFe_{0.9}Co_{0.1}AsF$) which is comparable with T_c in Co-substituted *R*FeAsO and AFe_2As_2.[19−21] These findings suggest the following possibilities. (1) Superconductivity in FeAs layers is insensitive to randomness compared with that in CuO_4 planes of high T_c cuprates.[22] (2) Superconductors with higher T_c still remain undiscovered in a large number of ZrCuSiAs and related type crystals.[23]

Samples were prepared by a solid state reaction of CaF_2 (99.99%), CaAs, Fe_2As, and Co_2As: $CaF_2 + CaAs + (1 - x)Fe_2As + xCo_2As \rightarrow 2CaFe_{1-x}Co_xAsF$. CaAs was synthesized by heating Ca shots (99.99 wt %) with As powder (99.9999 wt %) at 650 °C for 10 h in an evacuated silica tube. Fe_2As and Co_2As were synthesized from powders of mixed elements at 800 °C for 10 h (Fe, 99.9 wt %; Co, 99 wt %). These products were then mixed in stoichiometric ratios, pressed, and heated in evacuated silica tubes at 1000 °C for 10 h to obtain sintered pellets. All the starting material preparation procedures were carried out in an argon-filled glovebox (O_2, H_2O < 1 ppm). The analyzed Co concentration (*x*) by X-ray fluorescence analysis (Rigaku ZSX100e) utilizing the fundamental parameter method (see the Supporting Information) was confirmed to be almost the same as the nominal composition.

† Frontier Research Center.
‡ Materials and Structures Laboratory.
§ ERATO-SORST, JST.

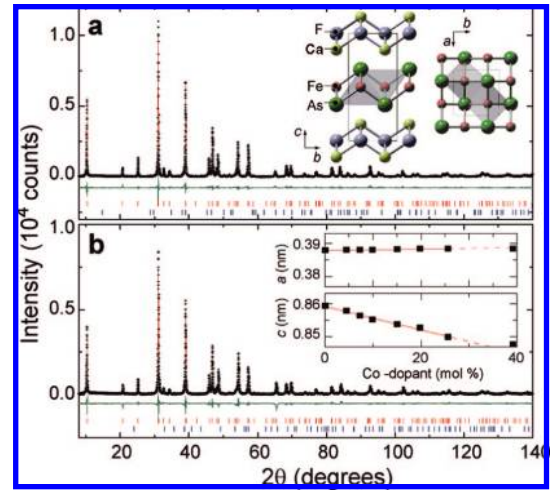

Figure 1. (a) Powder XRD patterns of CaFeAsF (+) and Rietveld fit (red line): Green line is difference between the patterns. Red and blue bars at bottom show Bragg diffraction positions calculated for CaFeAsF and Fe_2As. Inset shows structure model of CaFeAsF visualized by VESTA.[25] (b) XRD pattern of $CaFe_{0.9}Co_{0.1}AsF$. Inset shows lattice constants *a* and *c* as functions of Co content. Bars at bottom show calculated diffraction positions of $CaFe_{0.9}Co_{0.1}AsF$ and Fe_2O_3.

The crystal structure and lattice constants of the materials were examined by powder X-ray diffraction (XRD; Bruker D8 Advance TXS) using Cu K_α radiation with the aid of Rietveld refinement using Code TOPAS3.[24] The temperature dependence of DC electrical resistivity (ρ) at 2−300 K was measured by a four-probe technique using platinum electrodes deposited on samples. Magnetization (*M*) measurements were performed with a vibrating sample magnetometer (Quantum Design).

Figure 1 shows powder XRD patterns of undoped (a) and 10 atom % Co-substituted CaFeAsF (b). Main peaks are assigned to those of the CaFeAsF phase, and several weak peaks are assigned to Fe_2As for the undoped sample (the volume fraction is ∼2%) and Fe_2O_3 for the Co-substituted sample (1%). The CaFeAsF phase has tetragonal symmetry with room-temperature lattice constants of $a = 0.3878$ nm and $c = 0.8593$ nm for the undoped sample and $a = 0.3881$ nm and $c = 0.8552$ nm for the 10 atom % Co-substituted sample. As shown in the inset of Figure 1b, the *c*-axis length monotonically decreases with Co concentration below 26%, while the *a*-axis length remains almost constant. Since a Co substitution of 39% yields separation of the $CaCo_2As_2$ phase, the solubility limit of Co to the Fe site is estimated to be below 40%.

Figure 2a shows temperature (*T*) dependences of ρ and molar magnetic susceptibility (χ_{mol}) for undoped CaFeAsF. The $\chi_{mol}-T$ curve was obtained under a magnetic field (*H*) of 1 T with a zero field cooling (ZFC) mode. With a decrease in temperature, both $\rho-T$ and $\chi_{mol}-T$ curves exhibit sudden decreases at ∼120 K (T_{anom}).

10.1021/ja806357j CCC: $40.75

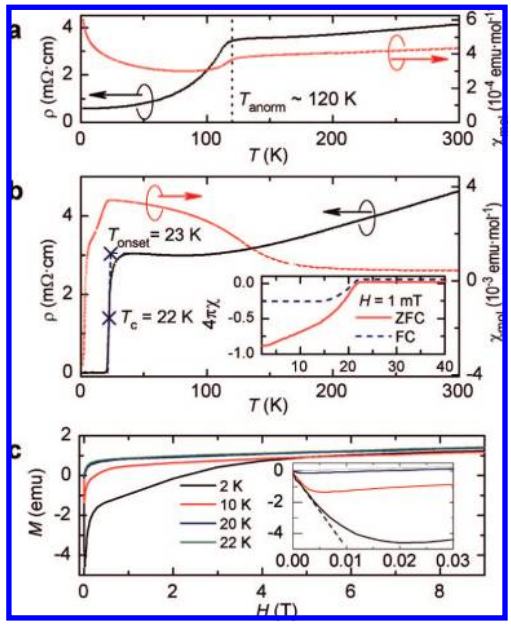

Figure 2. Electrical resistivity (ρ) and molar magnetic susceptibility (χ_{mol}) vs temperature (T) plots for undoped CaFeAsF (a) and $CaFe_{0.9}Co_{0.1}AsF$ (b). $\chi_{mol}-T$ plots were obtained under a magnetic field (H) of 1 T. Inset of (b) shows ZFC and FC $4\pi\chi-T$ plots (H = 1 mT) of $CaFe_{0.9}Co_{0.1}AsF$. (c) Magnetization (M) vs H plots for $CaFe_{0.9}Co_{0.1}AsF$. Expanded curves from 0 to 0.03 T are shown in the inset. The diamagnetic susceptibility was evaluated by the slope of linear region of $M-H$ curve (dashed line).

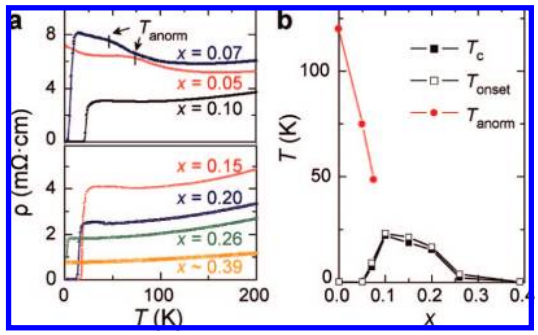

Figure 3. (a) $\rho-T$ plots for $CaFe_{1-x}Co_xAsF$: x = 0.05, 0.07, 0.10, 0.15, 0.20, 0.26, and ~0.39. (b) T_c and T_{onset} in the $\rho-T$ curves as a function of x. T_{anom} values for x = 0, 0.05, and 0.07 are also shown.

This behavior is quite analogous to those of RFeAsO and AFe$_2$As$_2$ that suffer crystallographic and/or magnetic transitions around T_{anorm}. As shown in Figure 2b, 10% Co substitution suppresses the anomalies and yields the abrupt decrease in ρ approaching zero. T_c defined as the temperature where the ρ value becomes half of that at the onset transition temperature (T_{onset} = 23 K) is 22 K. The observed increase in χ_{mol} at 22−180 K may be due to a small amount of ferromagnetic impurity such as FeAs:Co. The inset in Figure 2b shows volume susceptibility ($4\pi\chi$) vs T plots of $CaFe_{0.90}Co_{0.10}AsF$ under ZFC and field cooling (FC) with H = 1 mT. The diamagnetism due to superconductivity was observed below T_c. Figure 2c shows an $M-H$ plot for $CaFe_{0.9}Co_{0.1}AsF$. The volume fraction of the superconducting phase estimated from the diamagnetic susceptibility, which was obtained by the gradient of the linear region of $M-H$ curve, reaches up to 60% at 2 K.

Figure 3a shows $\rho-T$ curves for Co-substituted CaFeAsF samples with several x values. For x = 0.05 and 0.07, the anomaly appears as a shoulder and shifts to lower temperatures with an increase in x. Figure 3b summarizes T_{anorm} and T_{onset} as functions of x, demonstrating the Co substitution induces the superconducting phase in CaFeAsF and the highest T_c of 22 K is attained at x = 0.1. It is worth noting that the threshold and optimal electron-doping level are close to those of RFeAs($O_{1-x}F_x$) notwithstanding that the doped layer is different.

In summary, the electrical conductivity and magnetization measurements demonstrate Co-substituted CaFeAsF is a bulk superconductor. T_c changes with the Co content, exhibiting a maximum of 22 K at a Co content of ~10 atom %. We may expect a higher T_c if substitutional doping is successful to the $(CaF)^{\delta+}$ layer, since the T_c of Co-substituted CaFeAsF is higher than those of Co-substituted LaFeAsO (13 K) and SmFeAsO (15 K).[19,21]

Acknowledgment. We thank Dr. Sung Wng Kim and Takashi Mine of the Tokyo Institute of Technology and Dr. Youichi Kamihara of ERATO-SORST JST for their valuable discussions.

Note Added after ASAP Publication. Due to an error Figure 1 was replaced on October 29, 2008.

Supporting Information Available: Atomic compositions, powder X-ray diffraction patterns, lattice constants, and Rietveld analysis results. This material is available free of charge via the Internet at http://pubs.acs.org.

References

(1) Kamihara, Y.; Watanabe, T.; Hirano, M.; Hosono, H. *J. Am. Chem. Soc.* **2008**, *130*, 3296.
(2) Takahashi, H.; Igawa, K.; Arii, K.; Kamihara, U.; Hirano, M.; Hosono, H. *Nature* **2008**, *453*, 376.
(3) Chen, G. F.; Li, Z.; Wu, D.; Li, G.; Hu, W. Z.; Dong, J.; Zheng, P.; Luo, J. L.; Wang, N. L. *Phys. Rev. Lett.* **2008**, *100*, 247002.
(4) Ren, Z.-A.; Yang, J.; Lu, W.; Yi, W.; Che, G.-C.; Dong, X.-L.; Sun, L-L.; Zhao, Z.-X. *Mater. Res. Innov.* **2008**, *12*, 105.
(5) Ren, Z.-A.; Yang, J.; Lu, W.; Yi, W.; Shen, Z.-L.; Li, Z.-C.; Che, G.-C.; Dong, X.-L.; Sun, L.-L.; Zhou, F.; Zhao, Z.-X. *Europhys. Lett.* **2008**, *82*, 57002.
(6) Chen, X. H.; Wu, T.; Wu, G.; Liu, R. H.; Chen, H.; Fang, D. F. *Nature* **2008**, *453*, 761.
(7) Ren, Z.-A.; Lu, W.; Yang, J.; Yi, W.; Shen, X.-L.; Li, Z.-C.; Che, G.-C.; Dong, X.-L.; Sun, L.-L.; Zhou, F.; Zhao, Z.-X. *Chin. Phys. Lett.* **2008**, *25*, 2215.
(8) Wang, C.; Li, L.; Chi, S.; Zhu, Z.; Ren, Z.; Li, Y.; Wang, Y.; Lin, z.; Luo, Y.; Jiang, S.; Xu, X.; Cao, G.; Xu, Z. *Europhy. Lett.* **2008**, *83*, 67006.
(9) Rotter, M.; Tegel, M.; Johrendt, D. *Phys. Rev. Lett.* **2008**, *101*, 107006.
(10) Chen, G. F.; Li, Z.; Li, G.; Hu, W. Z.; Dong, J.; Zhang, X. D.; Zheng, P.; Wang, N. L.; Luo, J. L. *Chin. Phys. Lett.* **2008**, *25*, 3403.
(11) Wu, G.; Chen, H.; Wu, T.; Xie, Y. L.; Yan, Y. J.; Liu, R. H.; Wang, X. F.; Ying, J. J.; Chen, X. H. *J. Phys.: Condens. Matter* **2008**, *20*, 422201.
(12) de la Cruz, C, R.; Huang, Q.; Lynn, J. W.; Li, J.; Ratcliff, W., II; Zarestky, J. L.; Mook, H. A.; Chen, G. F.; Luo, J. L.; Wang, N. L.; Dai, P. *Nature* **2008**, *453*, 899.
(13) Nomura, T.; Kim, S.-W.; Kamihara, Y.; Hirano, M.; Sushko, P. V.; Kato, K.; Takata, M.; Shluger, A. L.; Hosono, H. arXiv:cond-mat/0804.3569.
(14) Margadonna, S.; Takabayashi, Y.; McDonald, M. T.; Brunelli, M.; Wu, G.; Liu, R. H.; Chen, X. H.; Prassides, K. arXiv:cond-mat/0806.3962.
(15) Wang, X. C.; Liu, Q. Q.; Lv, Y. X.; Gao, W. B.; Yang, L. X.; Yu, R. C.; Li, F. Y.; Jin, C. Q. arXiv:cond-mat/0806.4688.
(16) Hsu, F-C.; Yong Luo, J.-Y.; Yeh, K.-W.; Chen, T.-K.; Huang, T.-W.; Wu, P. M.; Lee, Y.-C.; Huang, Y.-L.; Chu, Y.-Y.; Yan, D.-C.; Wu, M.-K. arXiv: cond-mat/0807.2369.
(17) Mizuguchi, Y.; Tomioka, F.; Tsuda, S.; Yamaguchi, T.; Takano, Y. arXiv: cond-mat/0807.4315.
(18) Yeh, K.-W.; Huang, T.-W.; Huang, Y.-L.; Chen, T.-K.; Hsu, F.-C.; Wu, P. M.; Lee, Y.-C.; Chu, Y.-Y.; Chen, C.-L.; Luo, J.-Y.; Yan, D.-C.; Wu, M.-K. arXiv:cond-mat/0808.0474.
(19) Sefat, A. S.; Huq, A.; McGuire, M. A.; Jin, R.; Sales, B. C.; Mandrus, D. *Phys. Rev. B* **2008**, *78*, 104505.
(20) Sefat, A. S.; Jin, R.; McGuire, M. A.; Sales, B. C.; Singh, D. J.; Mandrus, D. *Phys. Rev. Lett.* **2008**, *101*, 117004.
(21) Qi, Y.-P.; Gao, Z.-S.; Wang, L.; Wang, D.-L.; Zhang, X.-Z.; Ma, Y.-W. *Supercond. Sci. Technol.* **2008**, *21*, 115016.
(22) Tarascon, J. M.; Greene, L. H.; Barboux, P.; McKinnon, W. R.; Hull, G. W. *Phys. Rev. B.* **1987**, *36*, 8393.
(23) Pottgen, R.; Johrendt, D. *Z. Naturforsch.* **2008**, *163b*, 1135.
(24) *TOPAS*, version 3; Bruker AXS: Karlsruhe, Germany, 2005.
(25) Momma, K.; Izumi, F. *J. Appl. Crystallogr.* **2008**, *41*, 653.

JA806357J